Electronic Supplementary Material (ESI) for Physical Chemistry Chemical Physics.

Comparison of the heat-treatment effect on carrier dynamics in TiO_2 thin films deposited by different methods

Ramsha Khan,*,†,§ Harri Ali Löytty,‡ Antti Tukiainen,¶ and Nikolai V. Tkachenko*,†,§

†*Photonic Compounds and Nanomaterials Group, Faculty of Engineering and Natural Sciences, Tampere University, P.O. Box 692, 33014 Tampere, Finland*

‡*Surface Science Group, Faculty of Engineering and Natural Sciences, Tampere University, P.O. Box 692, 33014 Tampere, Finland*

¶*Faculty of Engineering and Natural Sciences, Tampere University, P.O. Box 692, 33014 Tampere, Finland*

§*A shared footnote*

E-mail: ramsha.khan@tuni.fi; nikolai.tkachenko@tuni.fi

Phone: +358 40 7484160

1. Absorbance of flat films

1.1. An approximation of thin film and low absorbance

A common aim of absorption (spectra) measurements is to study sample absorbance or optical density. However, the propagation of the monitoring light through a film sample is affected not only by the sample absorbance, but also by reflectance from both surfaces of the film. In a standard solution measurements a reference sample with the same solvent but

free of the sample is used to solve the problem, but there is no such a reference sample when a film sample is measured. However, one can measure reflectance (spectrum) and use it to account for the reflectance "losses". If the film reflectance is R, then the relative intensity of the monitoring light is reduced by $1 - R$, and the relative light intensity after the sample is $(1 - R)10^{-A}$, where A is the film "true" absorbance also called optical density. Thus, the sample transmittance is

$$T = (1 - R)10^{-A} \tag{S1}$$

and the absorbance can be calculated from measured transmittance T and reflectance R spectra as

$$A = -\log\left(\frac{T}{1 - R}\right) \tag{S2}$$

It has to be noted that this is an approximation which does not account for

1. interference of the monitoring light inside the sample due to multiple reflections from both film surfaces,

2. absorption of light reflected from the back side of the film which reduces the total sample reflection.

The first problem starts to play a role when the film thickness approaches quarter of the wavelength. Since we work with 30 nm films we do not expect the interference to have strong impact on the measurements.

The second has vanishing impact in transparent samples, or at wavelengths > 400 nm in the case of TiO_2, which is the wavelength range of our main interest. And it will result in some overestimation of absorbance otherwise.

1.2. Steady state absorption spectra of flat films

The interference and reflection absorption can be accounted for but this requires more complex calculations. A model for accurate calculations of transmittance and reflectance spectra

of a semitransparent film deposited on transparent substrate was developed by Barybin and Shapovalov.[1] The sample structure is

air	film	substrate	air
	$\leftarrow d \rightarrow$		
$n = 1$	$n =$	$n = n_s$	$n = 1$
	$n_f + ik_f$		

Here the refractive index of the substrate is n_s, and the film has complex refractive index $n_f + ik_f$ with imaginary part, k_f responsible for the film absorption; k_f is also called extinction coefficient and it is directly proportional to the absorption coefficient $\alpha = \frac{4\pi k}{\lambda}$. The substrate is assumed to be thick enough so that the interference inside the substrate can be ignored. The transmittance and reflectance spectra, $T(\lambda)$ and $R(\lambda)$, can be calculated using eq. (43) in,[1] though the calculations and equations are bulky and we do not provide them here. The parameters needed for calculations are the film thickness, d, and spectra $n_f(\lambda)$, $k_f(\lambda)$ and $n_s(\lambda)$. We used single-term Sellmeier equation[2] to model refractive indexes of TiO_2 and quartz substrate

$$n(\lambda) = \sqrt{1 + \frac{\lambda^2}{B\lambda^2 - A}} \tag{S3}$$

where A and B are the constants specific to material and documented for a large variety of semiconductor and dielectric materials.[2] We have used $A = 1190$ and $B = 0.2182$ for TiO_2 anatase (wavelength in measured in nm) and amorphous TiO_2 was modelled by TiO_2 polyxtal with $A = 8400$ and $B = 0.207$.[2] The initial values for the substrate where take as fused silica but were adjusted to fit measured absorption spectra of our substrates and were $A = 6276.61$ and $B = 0.91851$.

This model is complemented by a factor accounting for possible sample porosity, namely the refractive index of the film is presented as[3]

$$n_f = (n - 1)p + 1 \tag{S4}$$

where n is the refractive index of the bulk material, e.g. TiO_2 anatase, and the parameter p is in the range $0 < p \leq 1$ where $p = 1$ corresponds to the layer without voids, and smaller p means larger effective volume of voids. Within this approximation the voids are assumed to be much smaller than the wavelength and homogeneously distributed through the film.

In order for the model to work well in the blue and near UV parts of the spectrum, one need to account for the sample absorption, $k_f(\lambda)$. This is especially important for as grown sample when the crystal structures is not well formed and the film has detectable absorption due to high degree of disorder and large number defects and trap states. To account for the rising sample absorption at wavelengths approaching the band gap the absorption extinction coefficient k_f was modelled by a step-like function having zero value at long wavelengths and approaching k_0 at short wavelengths

$$k = \frac{k_0}{\exp\left(\frac{\lambda-\lambda_0}{\triangle\lambda}\right) + 1} \tag{S5}$$

where λ_0 is the wavelength at the middle of transition from 0 to k_0 and $\triangle\lambda$ is the transition width (in the wavelength domain). Since the wavelength rage of our interest is above the wavelength corresponding the band gap, this equation will be used at $\lambda > \lambda_0$, meaning that we will observe only the long wavelength tail of the function.

1.3. Transient absorption (TA) measurements in transmittance and reflectance modes – estimation of the photoinduced absorbance change

The TA measurement were carried out in two modes, transmittance and reflectance, by measuring either transmitted part of the probe pulse of reflected part of the probe, but using a standard pump-probe instrument and in otherwise identical conditions, i.e. the same spot on the sample and the same excitation density and wavelength. In both cases the probe light intensity is measured and the saved signal is $-\log\left(\frac{\triangle I}{I}\right)$, where I is the light

intensity without excitation and $\triangle I$ is the difference in light intensities with and without excitation at a particular delay time. The transmittance mode is a standard method of TA pump-probe experiments, and the measured signals will be denoted as $\triangle A_T$. The results of reflectance mode TA measurements will be denoted as $\triangle A_R$.

Here we will consider a transient absorption responses of a thin film deposited on an optically thick substrate. The responses are affected by both absorption change and refractive index change and our aim is to estimate a "pure" absorbance change form two types of TA measurements, a traditional transmittance and complementary reflectance TA measurements carried out in identical conditions as described above. The studied samples are thin (close to 30 nm) relative to the monitoring wavelength, therefore we will neglect by the probe light interference in the samples due to multiple reflectance from the film interfaces, and use approximation provided by eq. (S1). This approximation can be further extended to the transient absorption case. Photo-excitation result in a change of all three values, T, R and A

$$T + \triangle T = (1 - R - \triangle R)10^{-A-\triangle A} = (1 - R - \triangle R)10^{-A}10^{-\triangle A} \tag{S6}$$

We are interested in $\triangle A$,

$$10^{-\triangle A} = \frac{T + \triangle T}{(1 - R - \triangle R)}10^{A} = \frac{T + \triangle T}{(1 - R - \triangle R)}\frac{1 - R}{T} = \frac{1 + \frac{\triangle T}{T}}{1 - \frac{\triangle R}{1-R}} \tag{S7}$$

Experimentally measured values are $\triangle A_T$ and $\triangle A_R$

$$\triangle T = T(10^{-\triangle A_T} - 1) \tag{S8}$$

$$\triangle R = R(10^{-\triangle A_R} - 1) \tag{S9}$$

therefore eq. (S7) can to be rearranged to

$$10^{-\triangle A} = \frac{(1 - R)\left(1 + \frac{\triangle T}{T}\right)}{1 - R\left(1 + \frac{\triangle R}{R}\right)} \tag{S10}$$

and

$$\triangle A = -\log\left[\frac{(1-R)10^{-\triangle A_T}}{1-R\,10^{-\triangle A_R}}\right] \tag{S11}$$

Within this approximation the absorbance change can be estimated from the measured reflectance spectrum of the sample, R, and TA measurements carried out in transmittance, $\triangle A_T$, and reflectance, $\triangle A_R$, modes. Before applying eq. (S11) to calculate $\triangle A$, the measured $\triangle A_T(\lambda, t)$ and $\triangle A_R(\lambda, t)$ arrays were converted to dispersion compensated data with common delay time base.

2. Distributed decay model

The relaxation dynamics of thin semiconductor films is often non-exponential even when the relaxation mechanism is simple and a "single step". We have used stretched exponential decay function[4] $f_s(t) = \exp\left[-\left(\frac{t}{\tau}\right)^{\beta}\right]$ to fit the TA decays but in many cases the stretching factor β was unreasonably small (< 0.3) generating initially fast decay below the time resolution of our instrument. To solve the problem we used distributed decay model with Gaussian distribution in logarithmic time constant scale

$$p(\tau) = \exp\left[-\frac{1}{2b^2}\left(\frac{\tau}{\tau_0}\right)^2\right] \tag{S12}$$

where τ_0 is the central decay time constant, and the factor b determines the width of the distribution in logarithmic scale, e.g. if $\tau_0 = 10$ ps and $b = 10$, then the decay time constant are spread between $\tau/b = 1$ ps and $\tau \times b = 100$ ps. This decay model provides better fit goodness compared to the stretched exponential, though the decay profiles looked rather similar.

3. Characterization

3.1. AFM

The height contrast images of all the as-deposited and HT samples along with RMS roughness values are presented in Fig. S1. Also, large scale (40×40 μm^2 area) AFM images of the heat treated SPD sample were measured. Large area analysis was done to ensure the adequate coverage of TiO_2 by spray pyrolysis technique. It can be seen from Figure S2a that TiO_2 covers all the surface but presents in form of overlapping round island like structures which most probably originates from spray pyrolysis droplets. Clearly, the number of overlapping islands is different at different locations and hence the thickness of TiO_2 is also different at different locations.

From GIXRD results in main text Fig. 3, assuming the shape factor of 1, the Scherrer equation applied to the (101) peaks which yielded the apparent crystallite sizes of 16 nm, 15 nm and 8 nm for ALD HT, IBS HT and SPD HT samples, respectively. The obtained values were comparable to the AFM results only in the case of SPD HT which had crystallite size smaller than the film thickness. For ALD HT and IBS HT, the crystallize size was an order of magnitude larger than the film thickness, while the apparent crystallite size derived from the XRD data was smaller than the film thickness.

3.2. Steady state spectra

The measured steady state transmittance and reflectance spectra of all samples are presented in Figure S3.

All the reflectance spectra have notable feature at roughly 850 nm. The origin of the feature is non-ideal reflectance of the reference mirror used to run base line of the spectrophotometer. To correct it, we used a clean quartz substrate (1 mm fused silica), recorded both transmittance, T and reflectance R spectra, and calculated "true" quartz reflectance spectrum as $R' = 1 - T$, as presented in Figure S4. Comparison of R and R' allows to calculate

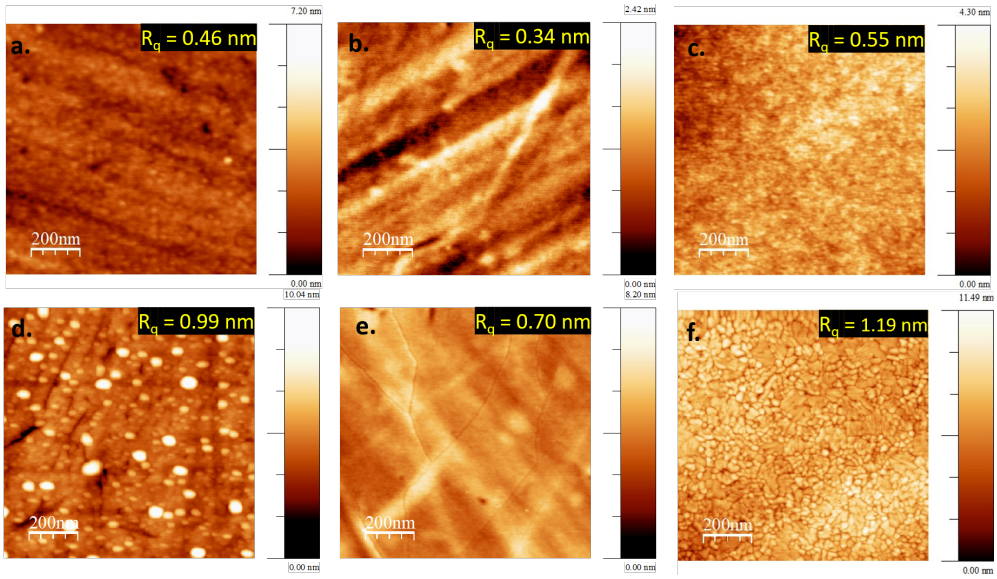

Figure S1: Nanoscaled AFM height profile images (1×1 μm^2 area) of as-deposited (a,b,c) ALD, IBS and SPD and heat-treated (d,e,f)ALD, IBS and SPD samples, respectively. The yellow values over figures are RMS roughness values

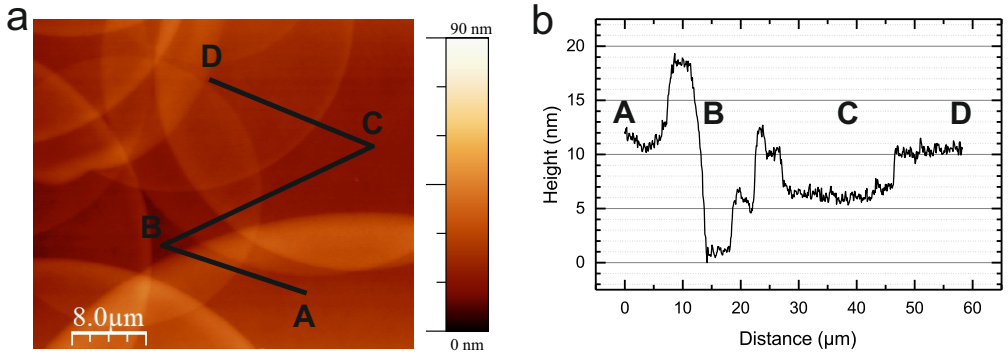

Figure S2: (a) 2D AFM image of HT SPD sample (40×40 μm^2 area) (b) roughness analysis of thickness of TiO_2 at different points of sample

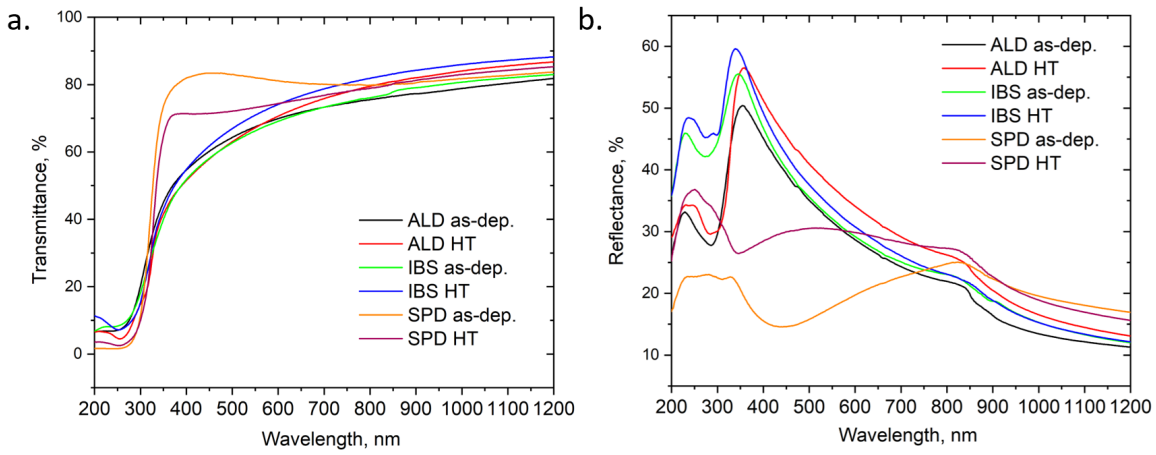

Figure S3: Steady state (a) Transmittance and (b) Reflectance spectra of 30 nm TiO_2 thin films deposited by ALD, IBS and SPD techniques

actual reflectance spectrum of the reference mirror marked in the figure as "mirror R".

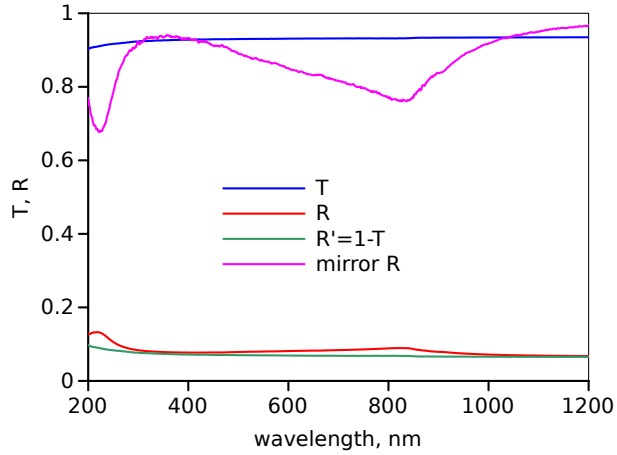

Figure S4: Measured transmittance T and reflectance R spectra of quartz substrate. $R' = 1 - T$ is the reflectance spectrum calculated from T assuming that quartz does not absorb any light in the wavelength range of measurements. Comparison of R and R' reveals the reference mirror reflectance spectrum marked as "mirror R".

The corrected reflectance spectra and measured transmittance spectra were used to calculate absorbance spectra shown in Fig. 1 of the main text using eq. (S2). The Tauc plot presentations of the same spectra in the photon energy range around the band gap are shown in Figure S5. These plots were used to estimate optical band gaps.

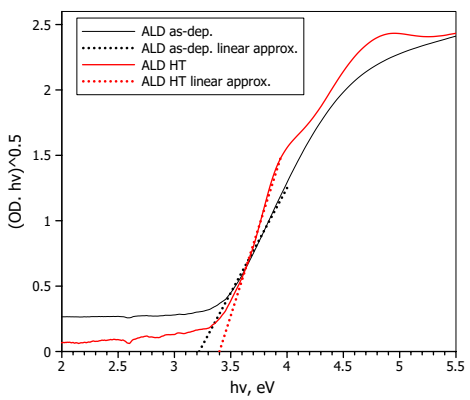

(a) ALD thin films

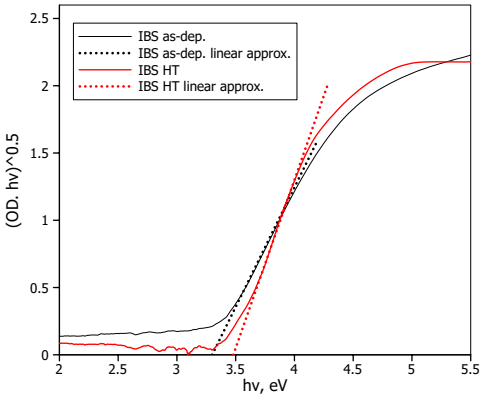

(b) IBS thin films

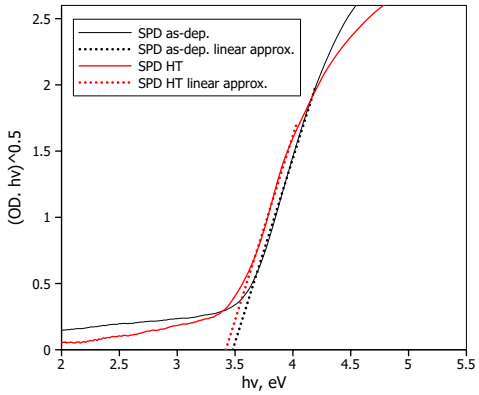

(c) SPD thin films

Figure S5: Tauc plots of TiO_2 thin films prepared by ALD, IBS and SPD, and slope linear approximations used to estimate optical band gaps.

4. Steady state absorption spectra modelling

The model given in Eq. S4 and Eq. S5 is applied to fit the measured absorbance spectra of the sample. The fitting parameters to model the measured absorbance spectra are p, the film thickness, d, and λ_0, $\triangle\lambda$ and k_0. The results of the fit for all samples are presented in Table S1 and summarized in the main text in Table 2.

Table S1: Absorption spectra fit parameters and the standard deviations (σ).

Sample	d, nm	p	$d \times p$, nm	λ_0, nm[a]	$\triangle\lambda$, nm	k_0	σ
ALD as deposited	90.4	0.66	59.4	452	97	0.4	0.0024
ALD HT	32.2	0.97	31.1	297	19	2.6	0.0015
IBS as deposited	23.1	1.05	24.3	320	21	1.3	0.0011
IBS HT	31.9	0.91	28.9	297	23	2.0	0.0013
SPD as deposited	94.6	0.58	55.2	275	104	0.3	0.0021
SPD HT	64.7	0.68	44.3	297	22	2.1	0.0057

[a] value of λ was fixed to 297 nm for HT samples to present correctly the band gap of anatase TiO_2.

The fit parameter $\triangle\lambda$ if relatively large for as-deposited ALD and SPD samples and it points out at remaining shallow absorption of the samples extended from the band gap region to the visible wavelength range. However, this is reasonable for amorphous TiO_2 which may be strongly contaminated by the precursor compounds and their decomposition products.

The model gives very good approximation of the measured spectrum for ALD HT sample with standard deviation of only 0.0015, and fit parameters come close to the expected values. Namely, the film thickness is 32.2 nm (intended thickness is 30 nm) and porosity factor $p = 0.97$, or virtually void free film. The sample absorption has an effect only at $\lambda <$ 360 nm which agrees well with TiO_2 anatase band gap. Absorption spectrum of as-deposited sample is clearly different from the HT one. One obvious reason for the difference is the film crystallinity, the as-deposited can by identified as amorphous and thus having different refractive index spectrum. The polyxtal TiO_2 n model[2] had to be complemented with porosity factor and absorption "tail" (eq. (S5)) to obtain a reasonable absorption spectrum approximation. However, the result has a straightforward explanation: the low temperature

ALD deposition does not result in formation of crystalline TiO_2 structure and has oxygen deficiencies with presence of precursor residuals, which leads to a tailing absorption in the visible part of the spectrum ($\triangle\lambda = 97$ nm) and also voids in the film ($p = 0.66$). The HT fixes both of these problems.

The absorption spectra of IBS and SPD samples were analysed in a manner similar to that described above for ALD samples. The resulting spectra, modelled A_{calc} and k are presented in Figs. S6 and S7, respectively. The IBS method results also in an amorphous film but it is much closer to TiO_2 than ALD, and the absorption spectra of as-deposited and HT samples are rather similar to each other (see Fig. S3). The most difficult for modelling turned out to be SPD samples (see Fig. S7). The large scale AFM imaging has shown that the problem is the film thickness homogeneity – the film looks as large number of overlapping disks with few tens on microns in diameter. However, at a qualitative level the difference between as-deposited and HT SPD samples is similar to that of ALD samples: HT removes tailing absorption in the visible and reduces film porosity.

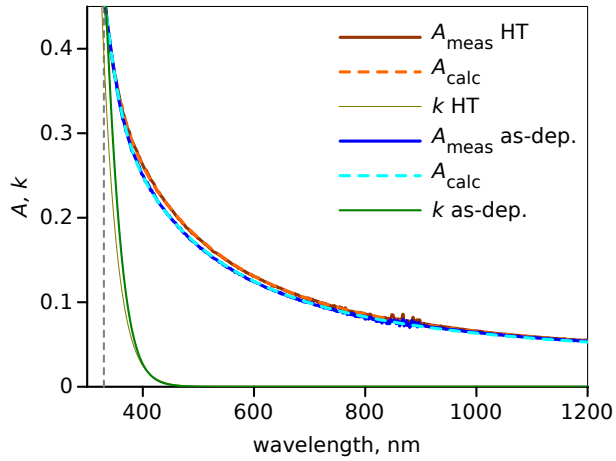

Figure S6: Measured A_{meas} and calculated A_{calc} absorption spectra of HT and as-deposited IBS samples, together with modelled absorption extinction coefficients k (imaginary part of refractive index.)

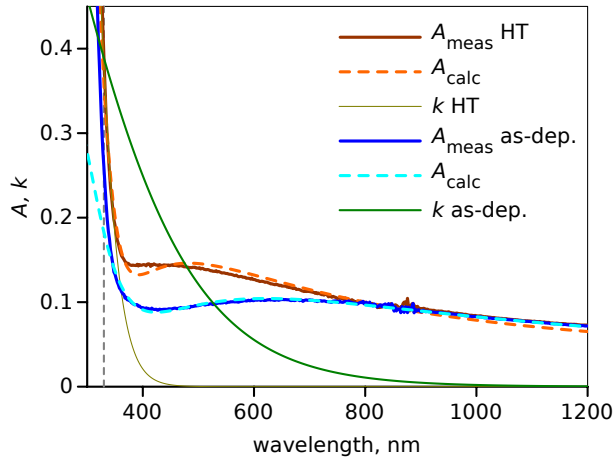

Figure S7: Measured A_{meas} and calculated A_{calc} absorption spectra of HT and as-deposited SPD samples, together with modelled absorption extinction coefficients k (imaginary part of refractive index.)

5. Transient absorption measurements and interpretation

The primary measured data in transmittance, $\triangle A_T(\lambda, t)$, and reflectance modes, $\triangle A_R(\lambda, t)$ were first recalculated to transient absorption (TA) response, $\triangle A(\lambda, t)$ using eq. (4). This TA data presents "true" absorption change and can be analysed using standard methods such as global (or multi-wavelength) data fitting. The aim of the global fitting is to obtain decay associated spectra (DAS) which can be used to calculate the species associated spectra (SAS), which in turn can be used to identify intermediate states. However, the practical implementation requires a mathematical model describing transition from one to another state. In the case of homogeneous system with thermally activated transitions the state populations follow (multi)exponential low, but the films are polycrystalline and composed of crystalline domains of different size, or they are intrinsically inhomogeneous. As the result, the (multi)exponential fitting may result in erroneous results. An empirical alternative is to use the so-called stretched-exponential instead, which often gives better results.[4] Yet another alternative we have tested is distributed decay model as described in Section 2. Different combination were tests to find the minimum number of component with the lowest

sigma value (average standard deviation between the data and fit). As an example, the fit model justification will be outlined for ALD as-deposited sample in the following section. It was found that all HT samples can be fitted using a fast (< 1 ps) exponential term, a exponential term with a few tens of ps time constant, and a long-lived distributed decay term. The ALD as-deposited sample required only distributed decay term, and two other as-deposited samples required a picosecond exponential and a longer-lived distributed decay terms.

5.1. TA measurements, $\triangle A$ calculations and fits

ALD as-deposited sample. Dispersion compensated raw measured TA data in transmittance, $\triangle A_T(\lambda, t)$, and reflected modes, $\triangle A_R(\lambda, t)$, are presented in Figs. S8a and S8b, respectively. The absorbance data, $\triangle A(\lambda, t)$, were calculated using eq. (S11) and the result is presented in Figs. S8c. This data were fitted using different decay models as presented in Table S2. There was a statistically significant increase in fit goodness (decrease in σ value) when switching from mono-exponential fit to bi-exponential fit, and only a minor improvement on switching to three exponential fit. However, the DAS spectra of all the components were virtually the same. A single component stretch-exponential fit gives virtually the same fit goodness as bi-exponential fit. This means that this data allow us to identify only one spectral component. The distributed decay model gives a minor, statistically insignificant σ value improvement, but since we observe somewhat better fit goodness with distributed decay for all samples the it is reported for all the samples. In conclusion, the TA data for ALD as-deposited sample can be finely fitted by a single distributed decay component with center time constant of 0.93 ± 0.03 ps, and the resulting decay associate spectrum (DAS) is shown in Fig. S8d.

IBS as-deposited sample. The raw TA measured data (after group velocity compensation), $\triangle A_T$ and $\triangle A_R$, calculated $\triangle A$, and $\triangle A$ fits are presented in Fig. S9. To obtain a

Table S2: Comparison of the fit results using different fit models for ALD as-deposited sample. Fit parameters are the time constant, τ, and stretched parameter, β, and the relative distribution width, b (eq.(S12)).

Fit model	fit goodness, σ (mOD)	fit parameters
one exponent	0.0439	$\tau_1 = 2.8$ ps
two exponents	0.0333	$\tau_1 = 1.2$ ps, $\tau_1 = 28$ ps
three exponents	0.0315	$\tau_1 = 0.7$ ps, $\tau_2 = 5.2$ ps, $\tau_3 = 110$ ps
stretched-exponent	0.0336	$\tau = 1.3$ ps, $\beta = 0.4$
distributed decay	0.0324	$\tau = 0.9$ ps, $b = 25$

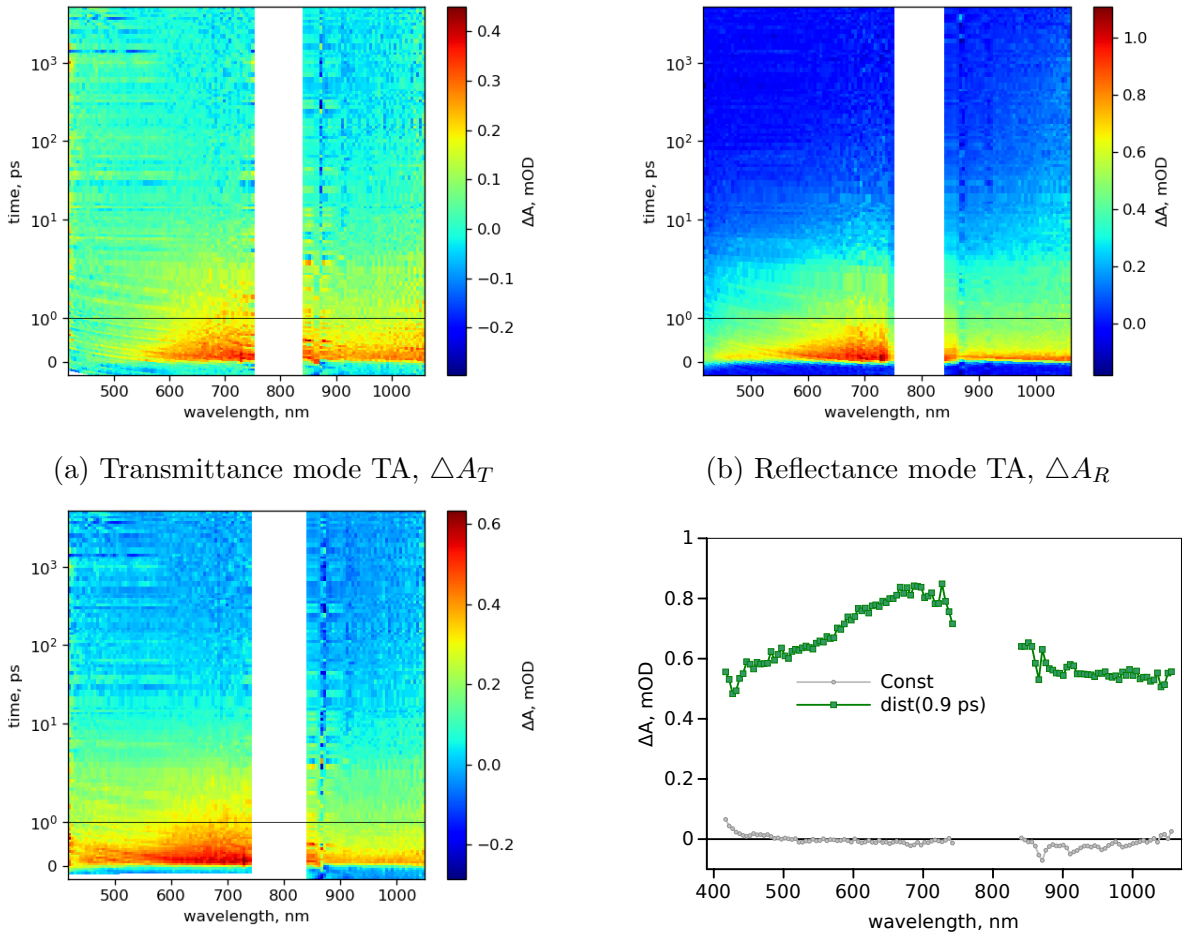

(a) Transmittance mode TA, $\triangle A_T$

(b) Reflectance mode TA, $\triangle A_R$

(c) Transient absorbance, $\triangle A$

(d) DAS

Figure S8: Color map presentation of the TA response of ALD as-deposited sample measured in (a) transmittance and (b) reflectance modes, and (c) calculated transient absorbance. The time scale is linear till 1 ps delay time and logarithmic after that. The excitation wavelength is 320 nm. (d) Decay associated spectrum.

reasonably good fit a sum of two exponential and distributed decays had to be used. One exponent time constant was 0.1 ps which is on the level of the instrument time resolution, most probably originated from the inaccuracy of dispersion compensation, and was ignored (not shown). Another exponent had 3.3 ps time constant and spectrum very similar to that of the distributed decay component with center time constant of 174 ps. There is virtually no spectrum shape change during the whole relaxation process.

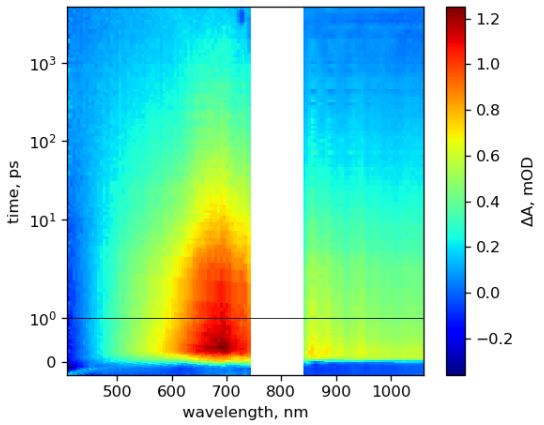

(a) Transmittance mode TA, $\triangle A_T$

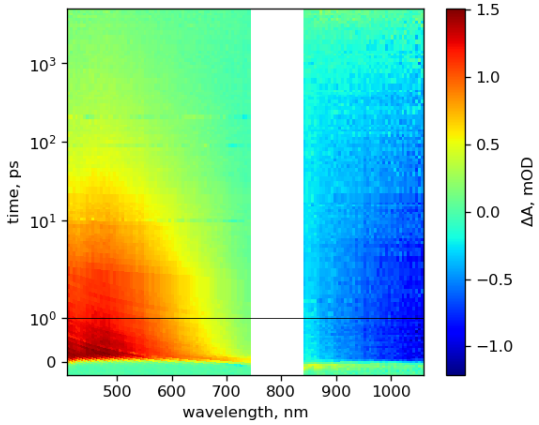

(b) Reflectance mode TA, $\triangle A_R$

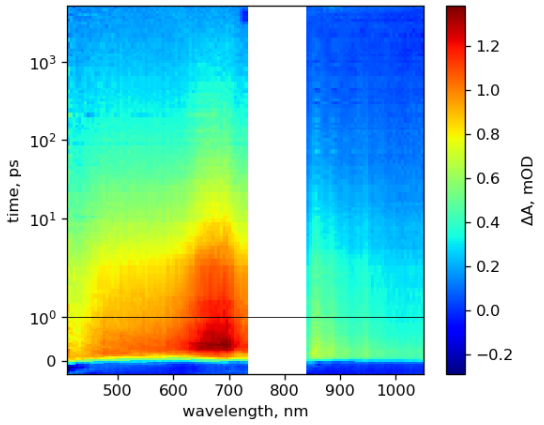

(c) Transient absorbance, $\triangle A$

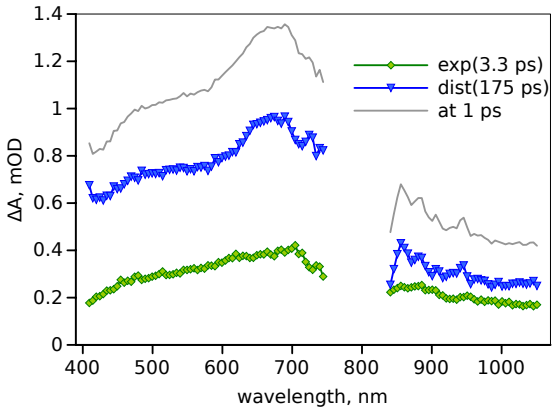

(d) DAS

Figure S9: Color map presentation of the TA response of IBS as-deposited sample measured in (a) transmittance and (b) reflectance modes, and (c) calculated transient absorbance. The time scale is linear till 1 ps delay time and logarithmic after that. The excitation wavelength is 320 nm. (d) Decay associated spectrum.

IBS HT sample. The raw TA measured data (after group velocity compensation), $\triangle A_T$ and $\triangle A_R$, calculated $\triangle A$, and $\triangle A$ fits are presented in Fig. S10. The fit model consisted of two exponential and distributed decays. Similar to other fits one exponential component had time constants shorter than the instrument time resolution (0.025 ps) and is ignored. The other exponential component had time constant of 53 ± 1 ps and the spectrum similar to that of 130 ps component of ALD HT sample.

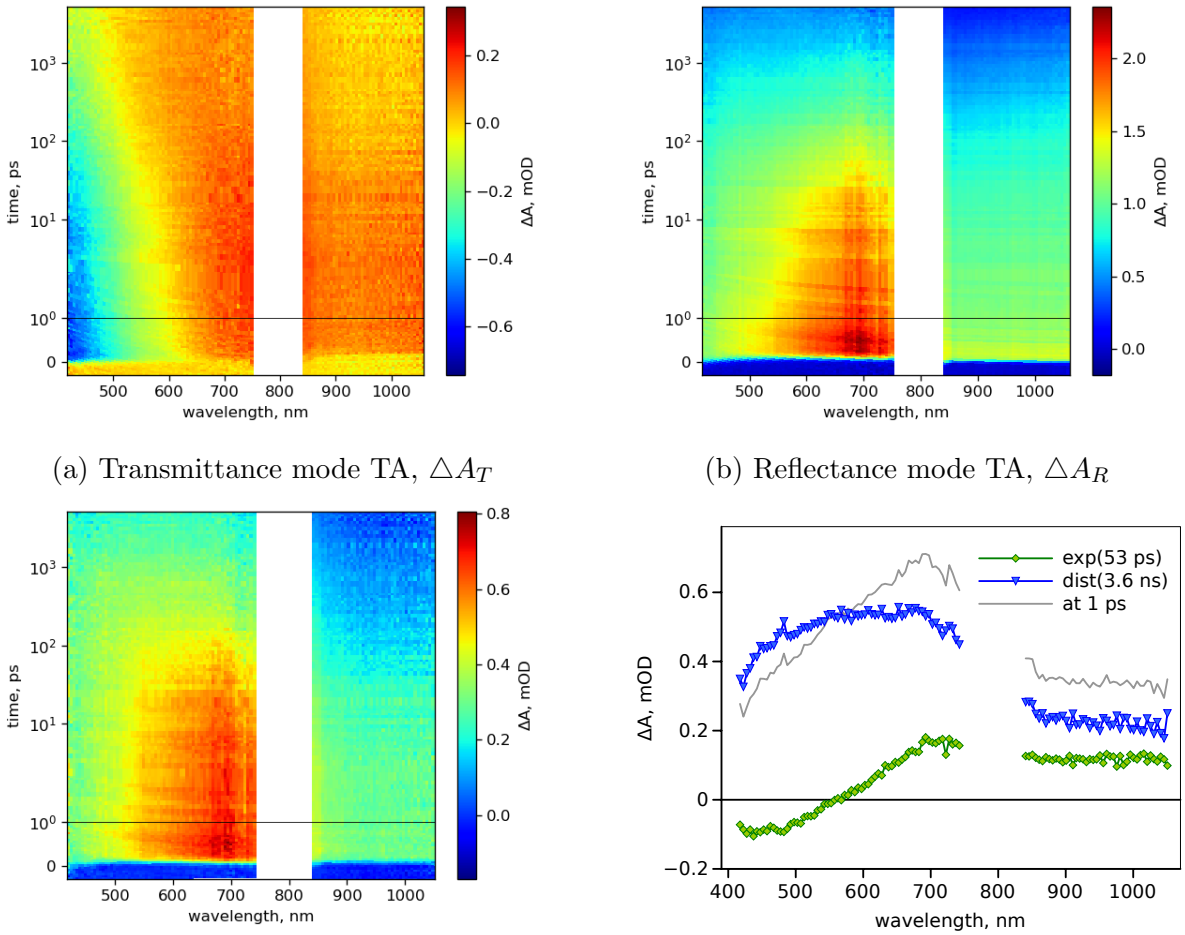

(a) Transmittance mode TA, $\triangle A_T$

(b) Reflectance mode TA, $\triangle A_R$

(c) Transient absorbance, $\triangle A$

(d) DAS

Figure S10: Color map presentation of the TA response of IBS HT sample measured in (a) transmittance and (b) reflectance modes, and (c) calculated transient absorbance. The time scale is linear till 1 ps delay time and logarithmic after that. The excitation wavelength is 320 nm. (d) Decay associated spectrum.

SPD as-deposited sample. The raw TA measured data (after group velocity compensation), $\triangle A_T$ and $\triangle A_R$, calculated $\triangle A$, and $\triangle A$ fits are presented in Fig. S9. To obtain a reasonably good fit a sum of exponential and distributed decays had to be used. The time constant of exponential component is 1.6 ps which is much sorter than the central time constant of the distributed decay, 50 ps, but the shapes of the components are only marginally different.

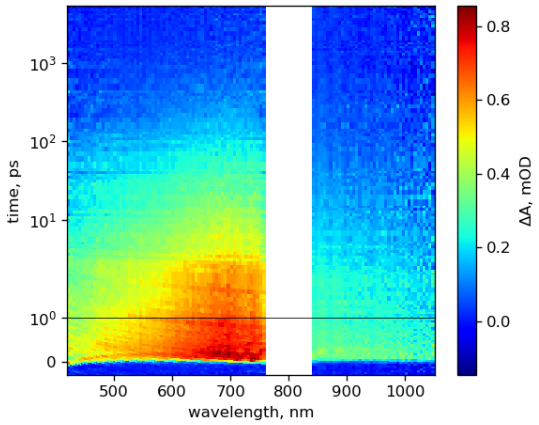

(a) Transmittance mode TA, $\triangle A_T$

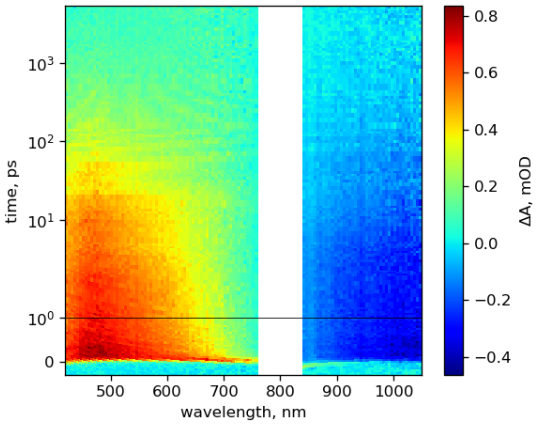

(b) Reflectance mode TA, $\triangle A_R$

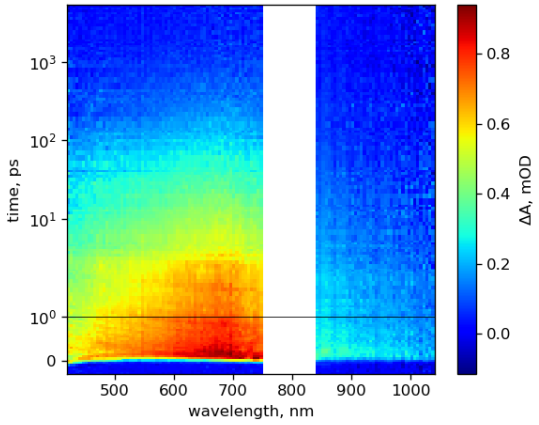

(c) Transient absorbance, $\triangle A$

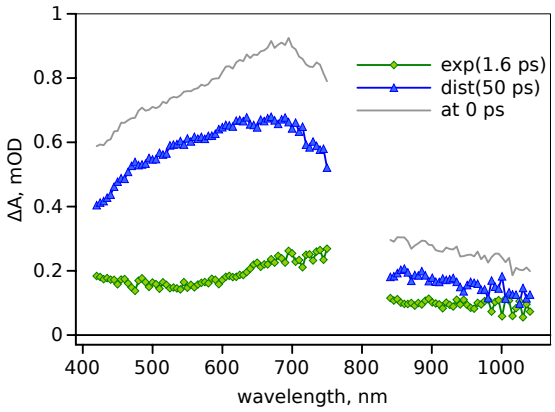

(d) DAS

Figure S11: Color map presentation of the TA response of SPD as-deposited sample measured in (a) transmittance and (b) reflectance modes, and (c) calculated transient absorbance. The time scale is linear till 1 ps delay time and logarithmic after that. The excitation wavelength is 320 nm. (d) Decay associated spectrum.

SPD HT sample. The raw TA measured data (after group velocity compensation), $\triangle A_T$ and $\triangle A_R$, calculated $\triangle A$, and $\triangle A$ fits are presented in Fig. S12. The fit model consisted of two exponential and distributed decays. Similar to other fits one exponential component had time constants close to the instrument time resolution (0.13 ps) and is ignored. The other exponential component had time constant of 98 ± 2 ps and spectrum similar to that of 130 ps component of ALD HT sample.

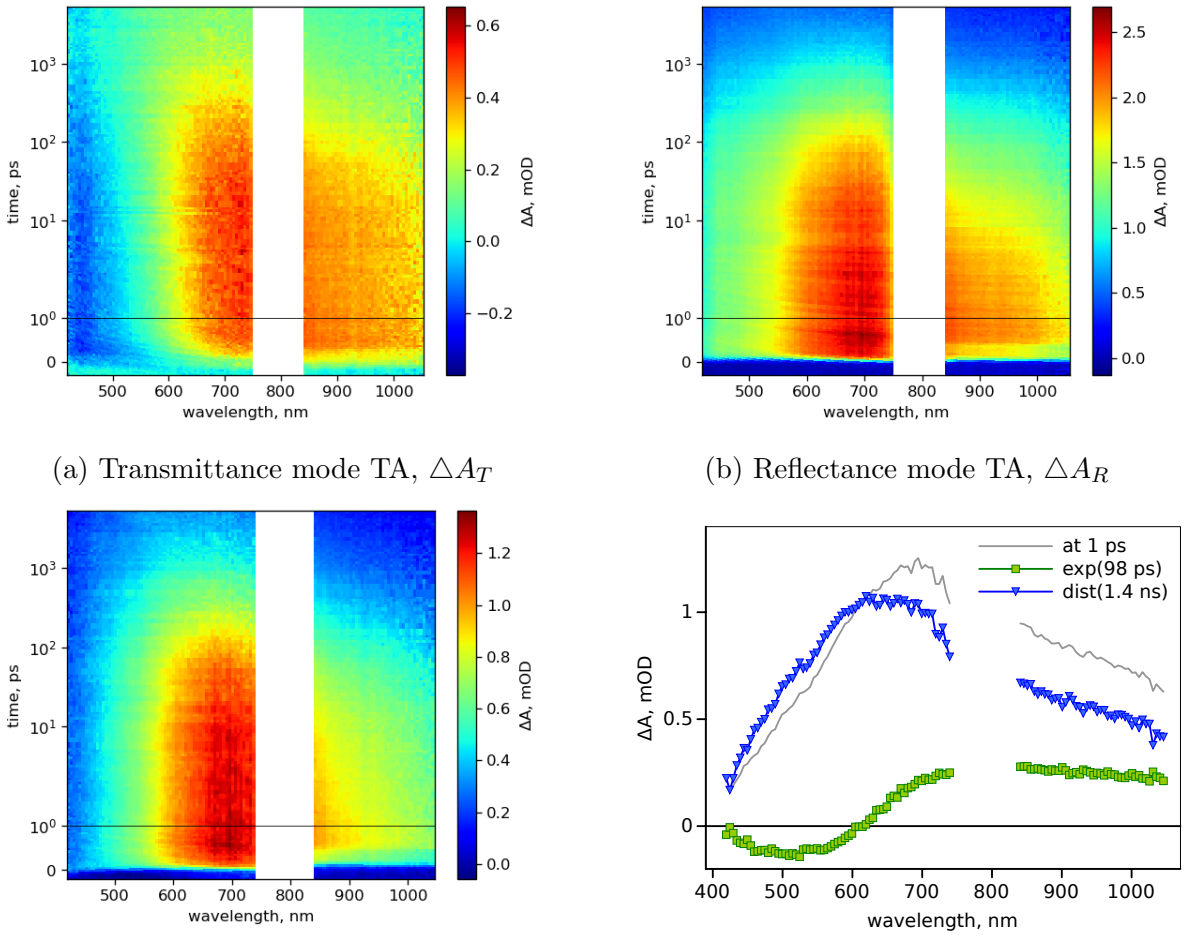

(a) Transmittance mode TA, $\triangle A_T$

(b) Reflectance mode TA, $\triangle A_R$

(c) Transient absorbance, $\triangle A$

(d) DAS

Figure S12: Color map presentation of the TA response of SPD HT sample measured in (a) transmittance and (b) reflectance modes, and (c) calculated transient absorbance. The time scale is linear till 1 ps delay time and logarithmic after that. The excitation wavelength is 320 nm. (d) Decay associated spectrum.

5.2. Lifetime of thicker samples

Thicker films of 200 nm were prepared by ion beam sputtering to study the effect of TiO_2 film thickness on the lifetime of different charge carrier components. The decay spectra of these samples were also fitted by two exponential and one distributed decay component. It was seen that increasing thickness of TiO_2 layer does not play any significant role in increasing the lifetime of photogenerated charge carriers and hence thicker films of TiO_2 will not provide any benefit to photocatalytic applications.

Table S3: Time constants for 200 nm as-dep. and HT IBS samples arising from global fit of the calculated $\triangle A(\lambda, t)$ data, τ_1 is exponential decay component, τ_d is distributed decay time constant and δ is the relative distribution width.

Samples	τ_1, ps	τ_d, ps (δ)
IBS as-dep.	3	30 (100)
IBS HT	56	1454 (69.1)

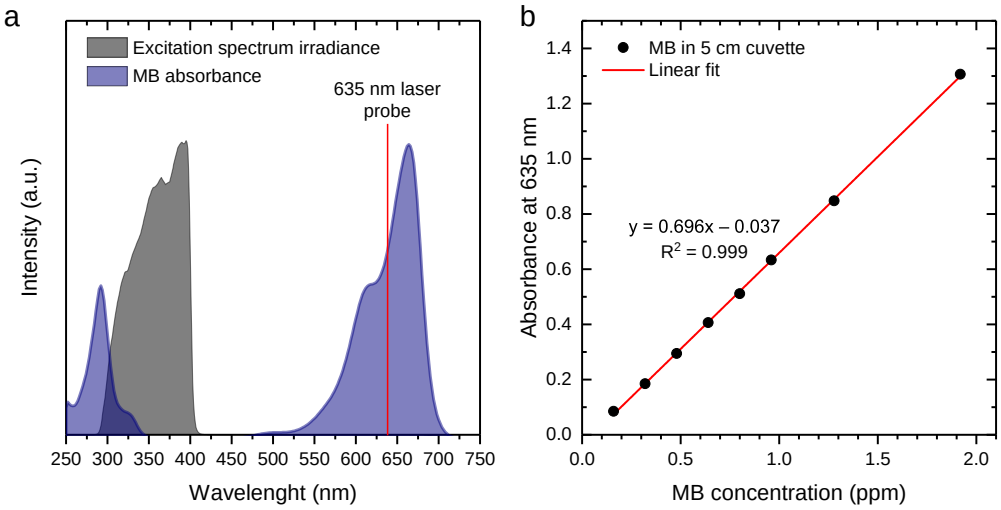

Figure S13: (a) Irradiance of the excitation light source, methylene blue (MB) absorbance and the wavelength of probe laser (bandwidth < 1 nm). (b) MB calibration curve measured in a cuvette with path length of 5 cm.

6. Methylene blue degradation

The excitation spectrum (300–400 nm) has only minor overlap with the methylene blue absorption spectrum as shown in Figure S13, and therefore, the filter effect in the test was small.

References

(1) Barybin, A.; Shapovalov, V. Substrate Effect on the Optical Reflectance and Transmittance of Thin-Film Structures. *Intern. J. Optics* **2010**, 137572.

(2) Shannon, R. D.; Shannon, R. C.; Medenbach, O.; Fischer, R. X. Refractive Index and Dispersion of Fluorides and Oxides. *J. Phys. Chem. Ref. Data* **2002**, *31*, 931–970.

(3) Santos, H. A. *Porous Silicon for Biomedical Applications*; 2014; pp 507–526.

(4) Berberan-Santos, M. N.; Borisov, E. N.; Valeur, B. Mathematical functions for the analysis of luminescence decays with underlying distributions 1. Kohlrausch decay function (stretched exponential). *Chem. Phys.* **2005**, *315*, 171–182.